Available online at www.sciencedirect.com
ScienceDirect
Ceramics International 37 (2011) 2679–2687
CERAMICS INTERNATIONAL
www.elsevier.com/locate/ceramint

Effect of silica doping on the densification and grain growth in zinc oxide

Tapatee Kundu Roy [a,*], Abhijit Ghosh [b,c], Debasis Bhowmick [a], Dirtha Sanyal [a], Soumyajit Koley [b], Alok Chakrabarti [a]

[a] *Variable Energy Cyclotron Centre, 1/AF Bidhan Nagar, Kolkata 700 064, India*
[b] *Bhabha Atomic Research Centre, Trombay, Mumbai 400 085, India*
[c] *School of Chemistry, University of St. Andrews, St. Andrews, Scotland KY16 9ST, UK*

Received 29 January 2011; received in revised form 9 April 2011; accepted 10 April 2011
Available online 15 April 2011

Abstract

The ability of silica (SiO_2) in controlling the densification and grain growth behavior of nano crystalline zinc oxide (ZnO) has been systematically studied. It has been observed that SiO_2 acts as a sintering inhibitor in the ZnO–SiO_2 system up to 4 wt.% limiting value beyond which densification behavior of the system remains almost unchanged, especially above 1100 °C. The addition of SiO_2 to ZnO retards grain growth which in turn results a finer ultimate grain size as compared to the undoped ZnO. However, stabilization in grain size occurs at ≥4 wt.% SiO_2 addition. It has been observed that SiO_2 incorporation changes the grain growth mechanism up to 4 wt.% addition, beyond which no remarkable changes was noticed. The grain growth (n) shows distinctly different slopes as a function of sintering time for the SiO_2 doped ZnO systems than undoped ZnO. The different slopes tend to indicate that different diffusion mechanisms and probably the formation of a secondary phase (Zn–Si–O) at the grain boundary control the densification and grain growth. The thermal expansion coefficient of the system has been found to decrease substantially beyond 4 wt.% SiO_2 addition to ZnO.

Keywords: A: Grain growth; A: Sintering; C: Thermal expansion; D: ZnO

1. Introduction

Zinc oxide (ZnO) based ceramics have generated great interest due to their possible use in various technological applications [1–5] viz., varistors, wide bandgap semiconductors, spintronics, various optoelectronic devices, etc. ZnO is also considered as a potential target material for the production of Radioactive Ion Beam [6,7]. An Isotope Separation On Line (ISOL) type RIB facility is being constructed at Variable Energy Cyclotron Centre, Kolkata, India. In an ISOL type RIB, radioactive atoms are produced inside thick targets by compound nucleus type nuclear reaction of the projectile beam with the target material. Diffusion is the underlying process by which the radioactive atoms come out of the target. The grain size is usually chosen to be a few micrometers [6] so that the radioactive atoms can diffuse out from inside the grain in a time not exceeding a few seconds, which is roughly equal to the half-lives of the radioactive atoms of interest. Since a typical experiment using RIB lasts for about a week, it is important that the grain size remains within the acceptable limit despite heating and consequent temperature rise in the target caused by long hours of beam irradiation. Therefore, to increase the overall applicability in various fields, a fine grain structure of sintered ZnO must be produced. To be more specific, the grain growth during sintering of ZnO should be controlled in order to have a fine grained structure.

Several studies have been conducted and reported in the literature [2,8–14] on the sintering and grain growth of ZnO systems with the addition of either single metal oxide or combination of different oxides viz., Bi_2O_3, Sb_2O_3, MnO–MnO_2, CuO, V_2O_5,CoO–Co_3O_4, SiO_2, etc. Senda et al. have studied various ZnO varistor systems [2,9] and found that Bi_2O_3 and Sb_2O_3 addition lowers grain growth. The addition of MnO [10] and V_2O_5 [13] have been observed to enhance the grain growth in ZnO system, whereas CuO [12] (only beyond 3 wt.%) and SiO_2 [14] addition prevent grain growth. Gunay et al. [15] studied the grain growth kinetics in ZnO–Bi_2O_3

* Corresponding author. Tel.: +91 3323184462; fax: +91 3323346871.
E-mail addresses: tapatee@vecc.gov.in, tapateekroy@yahoo.com (T.K. Roy).

0272-8842/$36.00
doi:10.1016/j.ceramint.2011.04.017

system with the addition of CoO as third component. In our initial work [7], we focused on the sintering and grain growth study of the undoped nanocrystalline ZnO powder (powder particle size ~30 nm) to understand its densification behavior over a range of temperature and time. This study showed that densification was much faster at 1300 °C and above and eventually became independent of holding time. Grain size also attained a saturation limit over sintering time at this temperature range. However, the grain size obtained after sintering at 1300 °C for 6 h was ~13 μm, which makes pure nanocrystalline ZnO powder unsuitable for its typical use as target material for the production and efficient release of radioactive products [6,7]. As a consequence, it became necessary to control the grain growth of nanocrystalline ZnO powder and limit the final grain size to a range of maximum 5 μm (decided by the half-life of the radioactive specie) after sufficiently long time of heating (~10 h) (in the grain growth stabilization zone).

In the present study, we emphasised to control the final grain size of ZnO samples within 4–5 μm after a prolonged heating (~10 h) at 1300 °C with the addition of minimum amount of SiO_2 as dopant. The minimum concentration of SiO_2 in ZnO is very important, otherwise it reduces the concentration of Zn atoms which in turn will affect the production of radioactive ion from Zn atom. The other important aspect of this study was to understand the influence of SiO_2 concentration on the grain growth mechanism of ZnO from a short heating duration (~5 min) to quite long (~10 h) heating time. The upper limit of temperature in the present study was restricted to 1300 °C. Above this temperature, increased volatility of ZnO makes it unsuitable for the use as target material in the production of RIB [6,7]. Another objective of the present investigation was to observe the change in thermal expansion coefficient of ZnO as a function of SiO_2 addition. This is necessary for ensuring the physical integrity of the target.

2. Materials and methods

2.1. Powder materials and characterization

ZnO (99.99%) and SiO_2 powder (99.99%) (both from Alfa Aesar, Johnson Matthey, Germany) were used as starting material in this study. ZnO powder (particle size ~0.1 μm) was ball-milled in a Fritsch Pulverissette 5 planetary ball mill grinder with agate balls for 30 h to achieve an average particle size of ~20 nm. Nanocrystalline ZnO powder was then mixed thoroughly with the required amount of SiO_2 powder (2–10 wt.%) in the ball mill grinder. Powder X-ray diffraction (XRD) study of nanocrystalline ZnO powder was carried out in a powder X-ray diffractometer (PW1710, Philips) with Cu Kα radiation with a Ni filter (λ = 1.5418 Å). Rate of scanning was kept at 0.02° step with a 3 s holding at each step. Crystallite size was estimated by an X-ray line broadening method considering broadening due to both strain and size factor using the modified Scherrer equation [16]:

$$(B^2 - B_{Si}^2)^{1/2} \times \cos\theta_B = 2\varepsilon \sin\theta_B + \frac{0.9\lambda}{L} \quad (1)$$

where L is the average crystallite size, ε is the strain and λ and θ_B denote the wave length of X-ray and Bragg diffraction angle, respectively. B and B_{Si} are total broadening and instrumental broadening, respectively. A highly diluted suspension of nano crystalline ZnO powder in isopropyl alcohol was taken on carbon grit for Transmission Electron Microscope (TEM, H600, Hitachi) observations. The BET surface area analysis of nano crystalline ZnO powder was performed using surface area analyzer (Sorptometric-1990, CE Instruments, Italy).

2.2. Densification

Sintering study was carried out with pellets compacted in a hydraulic pelletizer at 400 MPa pressure to a green density of 58–60% theoretical density (TD). These were heated (rate of heating: 600 °C/h) in a tubular furnace (Carbolite, UK) in air in the temperature range of 1000–1300 °C for different durations from 5 min to 10 h. Subsequently, the samples were furnace cooled. Bulk densities of the sintered specimens were determined by Archimedes liquid immersion technique [17] and expressed in terms of % TD. Variation in density values as measured was within ±1% of the same sample.

2.3. Microstructural study

Polished and etched surfaces of the sintered pellets were coated with a thin layer of Au–Pd alloy before examining in Scanning Electron Microscope, SEM (EVO 50, Carl Zeiss, UK). Spectrometric analysis was done with an Energy Dispersive Spectrometer, EDS (INCA PentaFETx3, Oxford Instruments, UK) attached with SEM. Grain size measurements were carried out on the micrographs using the following equation:

$$G = 1.56 \times L \quad (2)$$

where G is the average grain size, L is the average grain boundary intercept-length of four random lines drawn on two different micrographs of each sample [18].

2.4. XRD study of the sintered pellets

In order to characterize the phases present in the sintered specimens, XRD studies were carried out for a few ZnO–SiO_2 pellets (wt.% SiO_2 = 2, 4 and 6) sintered at 1000 °C and 1300 °C. The diffraction study was done using a Philips PW1710 diffractometer using Cu Kα radiation.

2.5. Thermal expansion measurement

A double push rod dilatometer (TD5000S, MAC Science, Japan) was used to determine the % thermal expansion and coefficient of thermal expansion (CTE) of the sintered samples in air in the temperature range of 200–900 °C.

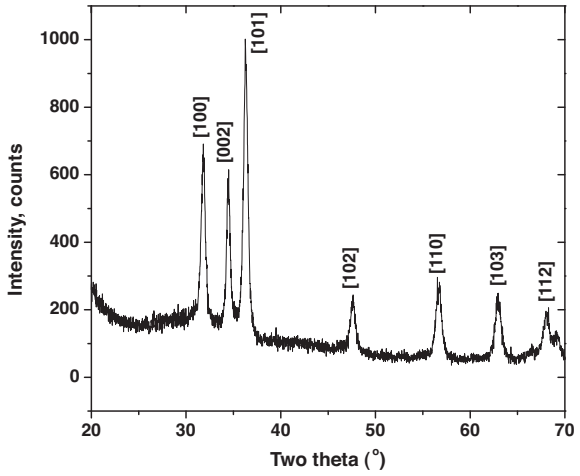

Fig. 1. X-ray diffraction pattern of nano crystalline ZnO powder.

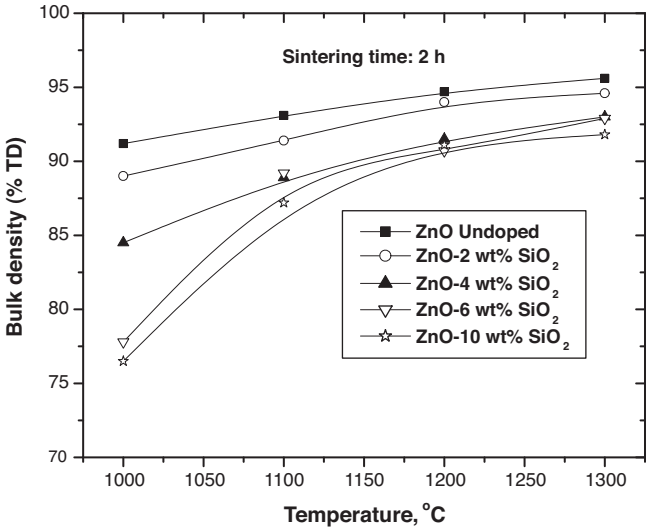

Fig. 3. Densification as a function of sintering temperature for undoped ZnO and ZnO–SiO_2 samples.

3. Results and discussion

3.1. Powder characteristics

The crystallite size of the ball-milled ZnO powder has been calculated from the broadened peaks of (1 0 0), (0 0 2), (1 0 1), (1 0 2), (1 1 0) and (1 03) of XRD spectra (Fig. 1) and found to be ~20 nm. Average particle size from the TEM image (Fig. 2) is found to be 20–30 nm and Brunauer–Emmett–Teller (BET) surface area of the same powder has been obtained as 43 $m^2\ g^{-1}$(equivalent spherical diameter, $d = 6/\rho S = 25$ nm, where ρ = TD = 5.65 g cm^{-3} for ZnO).

3.2. Sintering

The sintering behavior, i.e. the bulk density (% TD) of undoped ZnO (density 5.65 g cm^{-3}) and SiO_2 (density 2.65 g cm^{-3}) doped ZnO samples with the addition of different SiO_2 percentage (wt.%) is shown in Fig. 3. It indicates, for undoped ZnO, there is an increase in bulk density from 91% TD to >95% TD with increase in sintering temperature from 1000 °C to 1300 °C. SiO_2 is acting as a sintering inhibitor in the ZnO system, especially at lower temperature (1000 °C). The reason will be discussed in Section 3.4 with XRD study. It is also observed from Fig. 3 that the addition of SiO_2 beyond 4 wt.% limit yields an insignificant change in density in the ZnO system, especially at 1100 °C and above. Therefore, SiO_2 doping in ZnO reaches a limiting value at 4 wt.%. Beyond this limit, noticeable change in densification is not observed. Similar trend is observed in case of grain growth study as will be discussed in Section 3.5. In order to observe the changes in bulk density with sintering time, a few pellets have been sintered at 1300 °C with different holding times (up to 10 h).

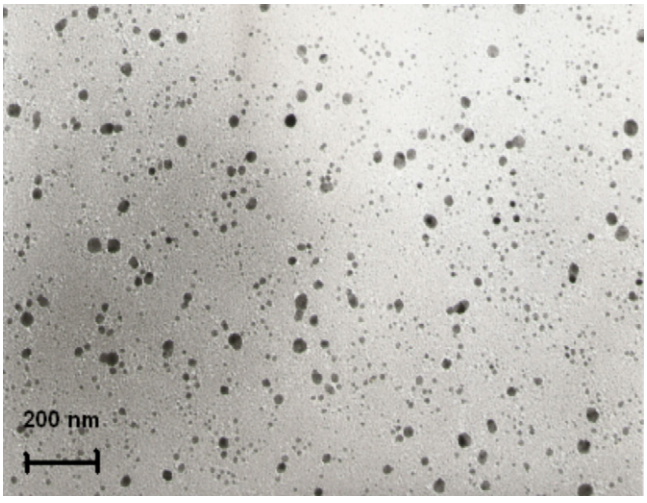

Fig. 2. TEM image of nanocrystalline ZnO powder.

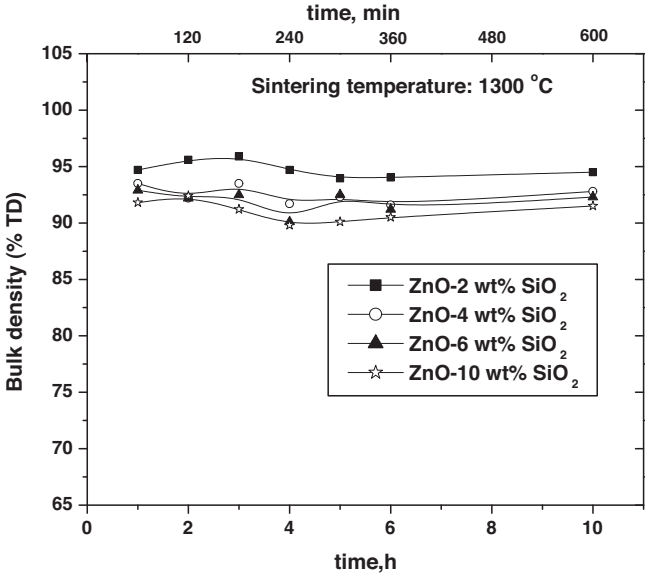

Fig. 4. Variation in bulk density with sintering time for ZnO–SiO_2 samples.

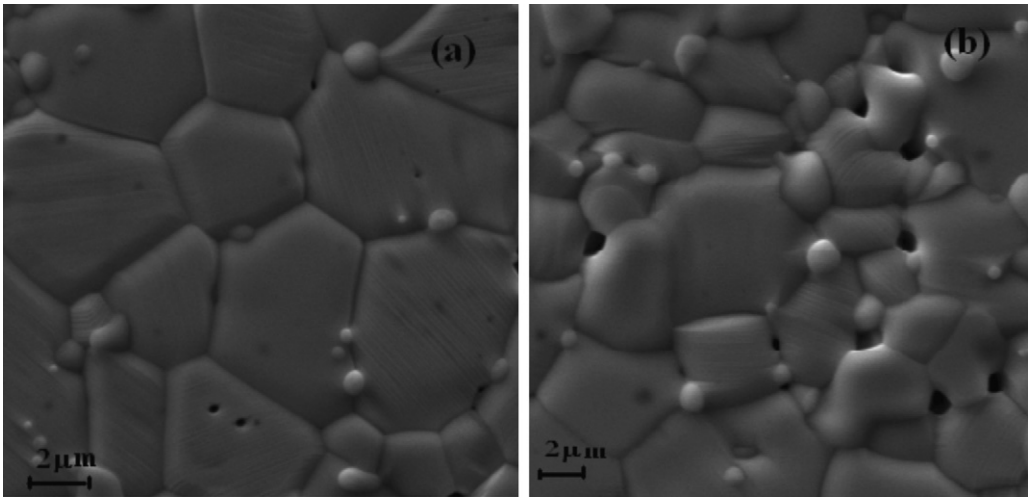

Fig. 5. SEM micrograph of polished and etched surface of (a) ZnO–2 wt.% SiO_2 and (b) ZnO–4 wt.% SiO_2 samples sintered at 1300 °C for 6 h.

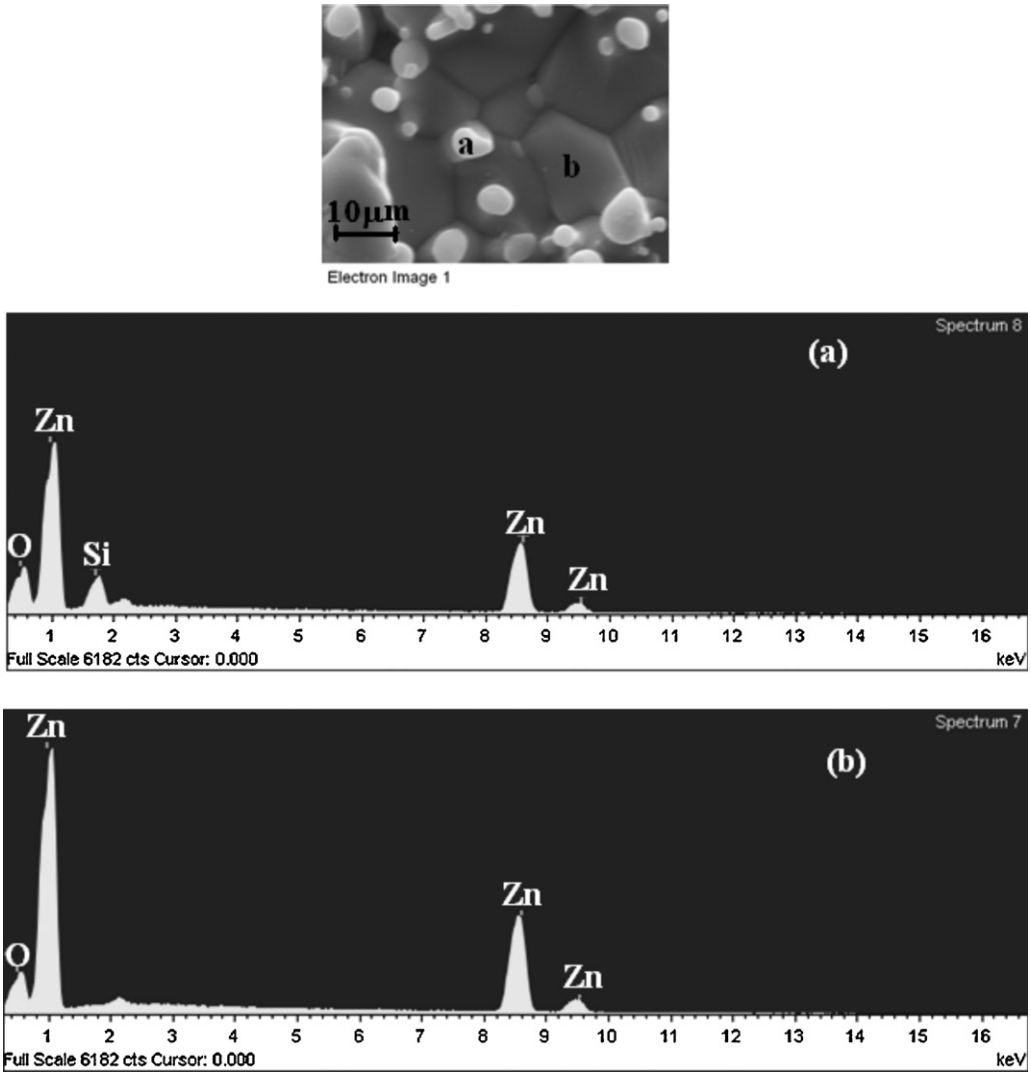

Fig. 6. EDS analysis of the microstructure showing distribution of zinc silicate phase.

The effect of sintering time on the densification behavior of undoped and SiO_2 doped ZnO pellets is plotted in Fig. 4. It shows that the variation in bulk density with time is negligible for each ZnO–SiO_2 composition within the present experimental range. This may be either due to the entrapment of pores within a grain structure, so that further densification by pore-removal becomes difficult, or due to the formation of a secondary phase preventing the diffusion process. In this study, probably the formation of less dense zinc silicate phase (Zn_2SiO_4, density 4.66 g cm^{-3}) explains the above observation.

3.3. Microstructure

Microstructures of SiO_2 doped ZnO pellets sintered at 1300 °C are shown in Fig. 5a and b. Prominent features observed in case of 2 wt.% added SiO_2 sample (Fig. 5a) are well defined grains along with a second phase mainly present in the grain boundary area. On increasing the SiO_2 doping to 4 wt.%, the change in grain size and density to a lower value is clearly observed in the micrograph. The distribution of the zinc silicate phases for the sample has been identified by EDS spectrometric analysis as shown in Fig. 6.

3.4. X-ray diffraction

In order to understand the temperature and required SiO_2 amount for the formation of zinc silicate phase, XRD analysis of ZnO–SiO_2 pellets sintered at and above 1000 °C is carried out and shown in Fig. 7a–d. As observed in Fig. 7b, the presence of zinc silicate phase (Zn–Si–O) becomes prominent at 1000 °C with the doping concentration of SiO_2 as 6 wt.%. In case of doping up to 4 wt.% SiO_2, this phase is not prominent when heated at 1000 °C (Fig. 7a). But it becomes visible as the sintering temperature increases to 1300 °C as observed for 2 wt.% SiO_2 sample (Fig. 7c). This means that the volume of Zn–Si–O phase formed at 1000 °C heated pellets up to 4 wt.% doping is below the detection limit of XRD. As the concentration of SiO_2 doping increases to 6 wt.%, the evidence of Zn–Si–O phase becomes visible even at 1000 °C. This may be the reason of significantly lowering the densification in case of ≥6 wt.% SiO_2 added samples at 1000 °C as observed in Fig. 3 and discussed in Section 3.2. However, at 1100 °C and above, saturation with respect to densification is observed for ≥4 wt.% SiO_2 added samples due to sufficient formation of Zn–Si–O phase to prevent diffusion during sintering. Indexing of XRD data shows the Zn–Si–O phase as Zn_2SiO_4 which matches with the observation of Canikoglu et al. [14] in their study.

3.5. Grain growth

Micrographs showing the change in grain sizes of ZnO–SiO_2 system with different SiO_2 percentages (0, 2, 4, 6 and 10 wt.%)

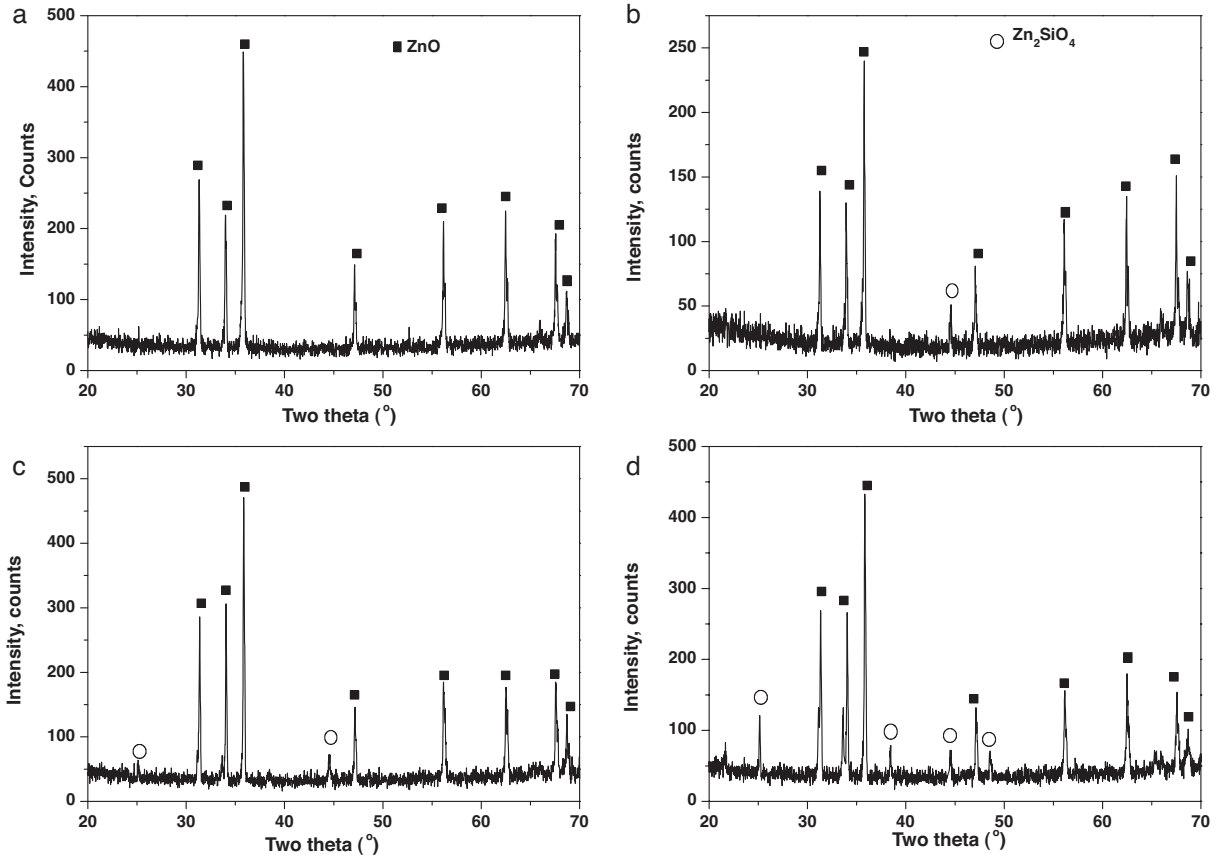

Fig. 7. X-ray diffraction pattern for ZnO–SiO_2 sintered samples (a) and (b) ZnO–4 wt.% SiO_2 and ZnO–6 wt.% SiO_2 samples, respectively, sintered at 1000 °C, (c) and (d) ZnO–2 wt.% SiO_2 and ZnO–6 wt.% SiO_2 samples, respectively, sintered at 1300 °C.

sintered at 1300 °C for 10 h are depicted in Fig. 8a–e. The average grain sizes (with its dispersion) of the samples sintered at 1300 °C (highest temperature) are drawn as a function of time in Fig. 9a for various weight percent of SiO_2. It is observed that the average grain size in undoped ZnO sintered at 1300 °C for 10 h is 20 μm. This size reduces to 13 μm with an addition of 2 wt.% SiO_2 to ZnO. The average grain size is of the order of 4–5 μm for SiO_2 concentration ≥4 wt.% in ZnO. Therefore, higher concentration of SiO_2 in excess of 4 wt.% is not required to control the grain growth of ZnO.

Studies on grain growth kinetics of ZnO [11–15] have revealed that the rate-controlling mechanism is the solid state diffusion of Zn^{2+} cations. The diffusion of Zn^{2+} cations or more explicitly the grain growth is strongly inhibited in SiO_2 doped

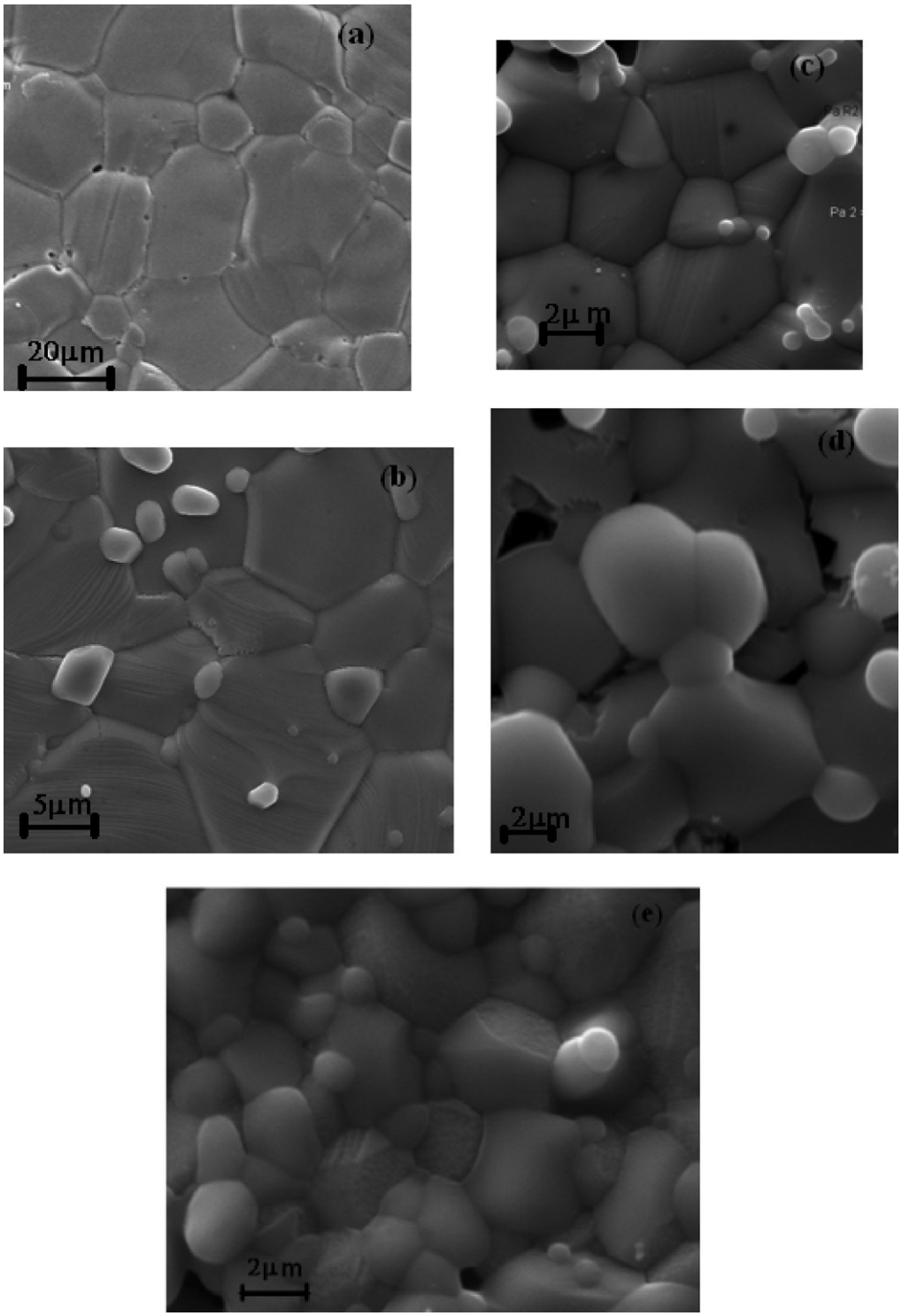

Fig. 8. Scanning electron micrograph of samples sintered at 1300 °C for 10 h: (a) undoped ZnO, (b) ZnO–2 wt.% SiO_2, (c) ZnO–4 wt.% SiO_2, (d) ZnO–6 wt.% SiO_2 and (e) ZnO–10 wt.% SiO_2.

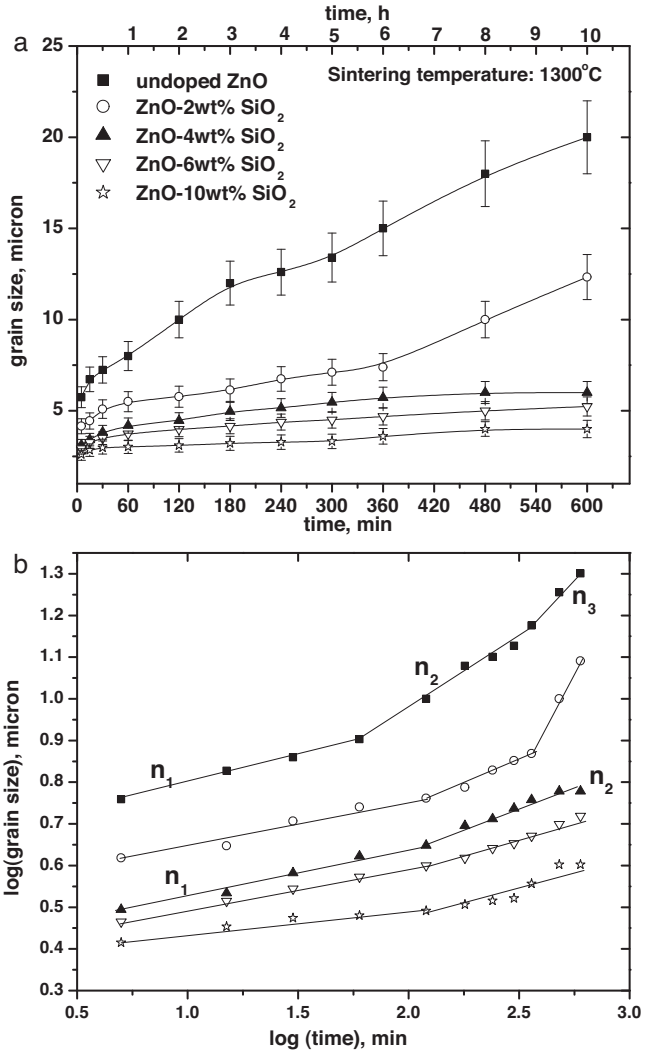

Fig. 9. Variation of grain size with sintering time in (a) normal scale and (b) logarithmic scale.

ZnO samples by the formation of Zn–Si–O phase in the grain boundaries.

The isothermal grain growth exponent, n was determined in order to throw some light on the grain growth mechanisms. Following Senda and Bradt [2], a simplified grain growth kinetics equation can be written as

$$G^n = kt \exp\left(\frac{-Q}{RT}\right) \quad (3)$$

where G is the average grain size at time t, n is the kinetic grain growth exponent, k is a constant, Q is the activation energy and R is the gas constant, T is the absolute temperature of sintering. The values of the grain growth exponent (n) as obtained from the slopes of log G versus log t plot (Fig. 9b) are listed in Table 1. The value of 'n' is found to be changing as a function of SiO_2 addition to ZnO system. The change in slope is due to the change in grain growth mechanism. In case of undoped ZnO, within first hour of sintering, the value of 'n' has been found to

Table 1
Slope of log d versus log t plot ($1/n$) and grain growth exponent (n) for undoped and SiO_2 doped ZnO.

Samples	Slope	n = 1/slope
Undoped ZnO	$Slope_1 = 0.13$	$n_1 = 8$
	$Slope_2 = 0.33$	$n_2 = 3$
	$Slope_3 = 0.56$	$n_3 = 2$
ZnO + 2 SiO_2	$Slope_1 = 0.11$	$n_1 = 9$
	$Slope_2 = 0.23$	$n_2 = 4$
	$Slope_3 = 1$	$n_3 = 1$, abnormal grain growth
ZnO + 4 SiO_2	$Slope_1 = 0.11$	$n_1 = 9$
	$Slope_2 = 0.18$	$n_2 = 5$
ZnO + 6 SiO_2	$Slope_1 = 0.09$	$n_1 = 10$
	$Slope_2 = 0.17$	$n_2 = 6$
ZnO + 10 SiO_2	$Slope_1 = 0.07$	$n_1 = 14$
	$Slope_2 = 0.17$	$n_2 = 6$

be around 8. This value further changes to the value of $n = 3$ (from 1 h to 6 h heating) matches with the results of the earlier workers [2,8]. This later value of 'n' signifies that the grain growth predominates via volume diffusion. For the first 1 h, the higher value of 'n' signifies a much slower rate of grain growth and the probable mechanism that occurs is surface diffusion [19], which requires a high proportion of free active surfaces. As the density of the sample reaches about ~95% TD (after 1 h) this process stops and grain growth proceeds via volume diffusion mechanism.

It is interesting to notice that SiO_2 doping in ZnO system is not only reducing the grain size, but also restricting the rate of grain growth. A close look at Fig. 9b indicates that the grain growth mechanism for all SiO_2 doped samples at the initial stage, i.e. up to 2 h ($\log t = 2.1$) may be governed by the surface diffusion mechanism, where the slope is low. Densification is less in SiO_2 doped ZnO than undoped ZnO and this may be a reason for surface diffusion to occur for longer duration (up to 2 h) in these samples as compared to undoped ZnO. At the intermediate stage, the mechanism of grain growth is varying depending on SiO_2 concentration from 2 wt.% to ≥4 wt.% in ZnO. In case of 2 wt.% SiO_2 doped sample, the value of 'n' is 4 from 2 h ($\log t = 2.1$) to 6 h ($\log t = 2.6$) heating. This value of 'n' signifies that grain boundary diffusion mechanism predominates in this region [19]. Beyond 6 h, different mechanisms might be operative, especially for undoped ZnO and 2 wt.% SiO_2 added to ZnO system. The rate of increase in the grain size at this region for these two compositions may indicate the presence of abnormal grain growth mechanism. However, the interesting observation is the stabilization of grain growth behavior for ≥4 wt.% SiO_2 added to ZnO composition. Even the grain growth mechanism remains same above 6 h of heating unlike undoped ZnO or 2 wt.% SiO_2 added sample. The microstructural features described earlier (Fig. 8) corroborates this observation. The value of 'n' = 5–6 for the sample containing ≥4 wt.% SiO_2 may be due to the presence of an appreciable amount of second phase (Zn–Si–O) segregating towards the grain boundary. This phase may have prohibited

mass transfer across the grain boundary and restricted the grain growth.

3.6. Thermal expansion

Linear thermal expansion ($\Delta L/L$) in percentage and coefficient of thermal expansion (CTE), $\alpha = dL/LdT$, as a function of temperature for ZnO pellets (both undoped and doped with SiO_2) are shown in Fig. 10. For all these samples, thermal expansion values increase monotonically over the entire range of measurement temperature. The CTE value of undoped ZnO pellet is around 6.51 ppm K^{-1} at 900 °C. The addition of 2 wt.% SiO_2 in ZnO does not make any change in the CTE value of ZnO. However, the addition of SiO_2 in amount of 4 wt.% reduces the CTE value of ZnO to 5.96 ppm K^{-1}. The value further reduces to 5.63 ppm K^{-1} when 6 wt.% SiO_2 is added in ZnO. It is well known that lower the value of CTE for any material, less will be the change in size of the material, when it is subjected to a temperature change. Therefore, the addition of SiO_2 in excess of 4 wt.% in ZnO is beneficial as it reduces the CTE value of ZnO.

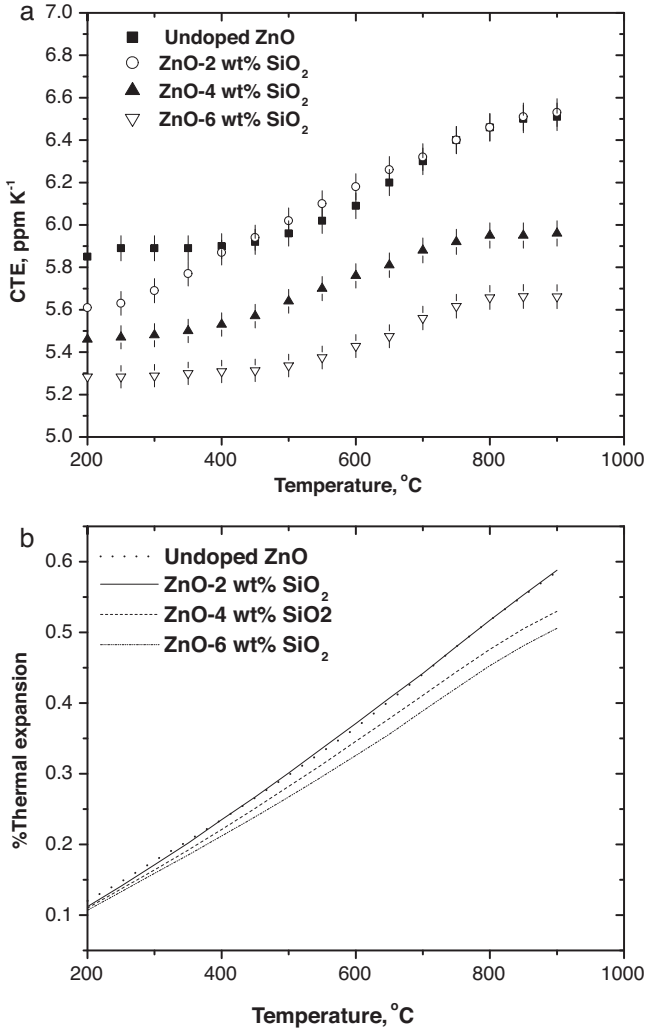

Fig. 10. Change of (a) CTE value and (b) percentage thermal expansion with temperature for both undoped ZnO and ZnO–SiO_2 samples.

4. Conclusions

Present study indicates that SiO_2 doping inhibits densification and grain growth in ZnO. However, beyond 4 wt.% addition of SiO_2 in ZnO, there is no significant change in the densification due to heating especially, at 1100 °C and above. The addition of SiO_2 ≥4 wt.% in ZnO limits the final grain size to 4–5 μm after heating for long time (∼10 h) at 1300 °C. It has been observed that grain growth has a strong dependence on percentage of SiO_2 addition, which, however, stabilizes beyond ≥4 wt.% SiO_2 addition. The final grain size comes down in SiO_2 doped ZnO samples possibly as a result of Zn–Si–O phase formation in the microstructure. Incorporation of SiO_2 ≥4 wt.% in ZnO also reduces the CTE value to 1 ppm K^{-1} at 900 °C. It is, therefore, established that SiO_2 doping in ZnO with a minimum amount of 4 wt.% helps in reducing the sintering and grain growth of ZnO which is one of the most important criteria for the use of ZnO as a target material in production of radioactive ions. This doping also helps in reducing the thermal expansion coefficient of ZnO.

References

[1] D.R. Clarke, Varistor ceramics, J. Am. Ceram. Soc. 82 (1999) 485–502.
[2] T. Senda, R.C. Bradt, Grain growth in sintering ZnO and ZnO–Bi_2O_3 ceramics, J. Am. Ceram. Soc. 73 (1990) 106–114.
[3] T. Dietl, H. Ohno, F. Matsukura, J. Gilbert, D. Ferrand, Zener model description of ferromagnetism in zinc-blende magnetic semiconductors, Science 287 (2000) 1019–1022.
[4] T. Pauporte, D. Lincot, Electrodeposition of semiconductors for optoelectronic devices: results on zinc oxide, Electrochim. Acta 45 (2000) 3345–3353.
[5] X. Wang, C.J. Summers, Z.L. Wang, Large scale hexagonal-patterned growth of aligned ZnO nanorods for nano-optoelectronics and nanosensor arrays, Nano Lett. 4 (2004) 423–426.
[6] D. Bhowmick, D. Naik, Md. Iqbal, D. Sanyal, S. DeChoudhury, V. Banerjee, A. Bandopadhay, P. Deb, D. Bhattacharya, A. Chakrabarti, Preparation and optimization of targets for the production of radioactive ions at VECC, Nucl. Instrum. Meth. Phys. Res. Sect. A: Accel. Spectrom. Detect. Assoc. Equip. 539 (2005) 54–62.
[7] Tapatee K. Roy, D. Bhowmick, D. Sanyal, A. Chakrabarti, Sintering studies of nano crystalline zinc oxide, Ceram. Int. 34 (2008) 81–87.
[8] J.E. Burke, D. Turnbull, Recrystallization and grain growth, Prog. Metal. Phys. 3 (1952) 220–292.
[9] T. Senda, R.C. Bradt, Grain growth of zinc oxide during the sintering of zinc oxide-antimony oxide ceramics, J. Am. Ceram. Soc. 74 (1991) 1296–1302.
[10] J. Han, P.Q. Mantas, A.M.R. Senos, Grain growth in Mn doped ZnO, J. Eur. Ceram. Soc. 20 (2000) 2753–2758.
[11] O. Toplan, V. Gunay, O.T. Ozkan, Grain growth in MnO added ZnO–6 wt%Sb_2O_3 ceramic system, Ceram. Int. 23 (1997) 251–255.
[12] F. Apaydin, H.O. Toplan, K. Yildiz, Effect of CuO on the grain growth of ZnO, J. Mater. Sci. 40 (2005) 677–682.
[13] H.H. Hng, L. Halim, Grain growth in sintered ZnO–1 mol% V_2O_5 ceramics, Mater. Lett. 57 (2003) 1411–1416.
[14] N. Canikoglu, N. Toplan, K. Yildiz, H. Ozkan Toplan, Densification and grain growth of SiO_2 doped ZnO, Ceram. Int. 32 (2006) 127–132.
[15] V. Gunay, O. Geleck-Sulan, O.T. Ozkan, Grain growth kinetic in xCoO–6 wt% Bi_2O_3–(94−x) ZnO (x = 0, 2, 4) ceramic system, Ceram. Int. 30 (2004) 105–110.

[16] G.K. Williamson, W. Hall, X-ray line broadening from filed aluminum and wolfram, Acta Metall. 1 (1953) 22–31.
[17] ASTM Designation: C830-88 Standard Test Methods for Apparent Porosity, Liquid Absorption, Apparent Specific Gravity, and Bulk Density of Refractory Shapes by Vacuum Pressure, Annual Book of ASTM Standards, ASTM, Philadelphia, PA, 1988.
[18] eighth ed., Metals Handbooks, vol. 8, American Society for Metals, Warrandale, PA, USA, 1973.
[19] R. El-Khozondar, H. El-Khozondar, G. Gottstein, A. Rollet, Microstructural simulation of grain growth in two-phase polycrystalline materials, Egypt. J. Solids 29 (2006) 35–47.